ELSEVIER

Surface Science 329 (1995) L593–L598

surface science

Surface Science Letters

Electron-stimulated oxidation of Ni(111) at low temperature

Wei Li, M.J. Stirniman, S.J. Sibener *

The James Franck Institute and Department of Chemistry, The University of Chicago, 5640 South Ellis Avenue, Chicago, IL 60637, USA

Received 16 January 1995; accepted for publication 20 February 1995

Abstract

We have found that electron beams from 5 eV to 2 keV stimulate facile nickel oxide growth on Ni(111) at 120 K, and that oxidation occurs extremely slowly at low temperatures when electron irradiation is absent. These results differ significantly from previous studies, discrepancies which can be attributed to synergistic effects involving electrons. A model is proposed which quantitatively accounts for the data and yields relevant cross sections. These findings are of fundamental importance to metallic oxidation and corrosion, and may find application in electron beam and STM lithography.

Keywords: Auger electron spectroscopy; Electron energy loss spectroscopy; Models of surface kinetics; Molecule–solid reactions; Nickel; Nickel oxides; Oxidation; Oxygen

Metallic oxidation and corrosion are phenomena of central importance to interfacial chemistry and materials science. In this Letter we report recent findings which demonstrate that synergistic effects involving electrons, oxygen, and the Ni(111) surface at low substrate temperature can lead to significant changes in the oxidation chemistry of this interface. Low temperature studies of nickel oxidation are rather scarce, and are in general agreement that oxygen uptake proceeds through a rapid chemisorption stage, followed by oxide nucleation and growth to a saturation thickness of approximately three layers [1–3], similar to the saturation coverage at room temperature [1–5].

In the present work, we have carefully reinvestigated Ni(111) oxidation at 120 K. We have discovered, in contrast to previous work [1], that at this temperature nickel oxide growth proceeds extremely slowly (if at all) after completion of an initial oxygen chemisorption stage. We present clear evidence that explains this important discrepancy, namely that electrons stimulate the oxidation of Ni(111) at low temperature. A mechanistic model is proposed which quantitatively accounts for the data and yields relevant cross sections for the electron-stimulated oxidation of this interface. These findings have obvious and important implications for other systems. Electron irradiation either *during* oxygen exposure, or *alternating* with it, can lead to this effect, indicating that the electron beam creates nucleation centers for nickel oxide growth.

The ability of electrons to perturb experimental systems such that they deviate from their typical behavior has been well documented in the literature. One of the most obvious situations is when electron bombardment can induce damage or structural change

* Corresponding author. E-mail: sibener@silly.uchicago.edu Fax: +1 312 702 5863.

SSDI 0039-6028(95)00352-5

at an interface, as has been reported for low energy electron diffraction (LEED) studies for many years [6]. More directly related to this study are instances where electrons provide a powerful method of stimulating physical and chemical effects and establishing new phenomena: electrons can stimulate desorption [7], adsorption [8], dissociation [9], migration [10], and oxidation [11,12]. These effects clearly show that electrons have the capability to modify the nascent phenomena being investigated, at times so markedly that the conclusions drawn may not be directly applicable to the unperturbed system. This paper will demonstrate that this can be particularly troublesome when studying oxidation/corrosion reactions with electron-based probes.

The experiments were carried out in a UHV system (base pressure 7×10^{-11} Torr) which has been previously described [13]. This apparatus has several surface diagnostics which have been used in this study, including LEED, Auger electron spectroscopy (AES), and high resolution electron energy loss spectroscopy (HREELS). The Ni(111) sample was oriented to within $\pm 0.2°$ and prepared by repeated cycles of Ar^+ ion sputtering and annealing at 1100 K. Oxygen was admitted to the UHV chamber for background dosing at pressures of 3×10^{-8} to 3×10^{-7} Torr. Electron irradiation of the sample utilized the electron guns of the Auger spectrometer (for $E > 500$ eV) and LEED system (for $E < 500$ eV). Beam current at the target was measured with the sample biased at $+94$ V to minimize secondary emission.

The observations which triggered the present work are shown in Fig. 1. Here we measured the oxygen uptake of a Ni(111) surface at 120 and 270 K with AES. Data were collected using three different procedures: In the first case (Fig. 1a, solid triangles) the sample was simultaneously exposed to both oxygen and an electron beam from the Auger system's electron gun. Auger spectroscopy measurements were then performed at various exposure times in order to assess the extent of oxygen uptake by the sample. In the second case data were obtained by first dosing the sample to the desired oxygen exposure, and then measuring the oxygen content of the sample with AES at 120 and 270 K, Fig. 1a open diamonds and squares, respectively. Then, before adsorbing oxygen to the next desired total oxygen exposure, the sample

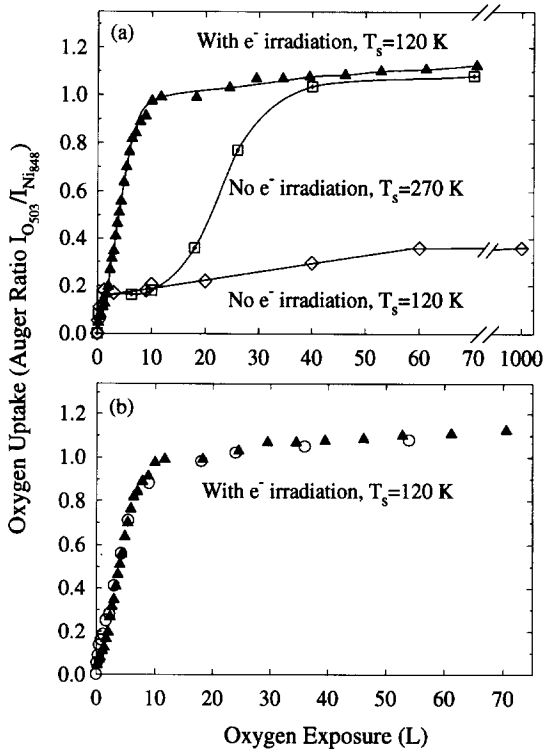

Fig. 1. Oxygen uptake versus oxygen exposure under various experimental conditions. (a) Solid triangles: oxygen uptake during simultaneous exposure of the surface to both electrons and oxygen at 120 K; open diamonds and squares: oxygen uptake without electron exposure at 120 and 270 K; (b) oxygen uptake versus oxygen exposure with the sample at 120 K and simultaneously (solid triangles) or alternately (open circles) exposed to electrons and oxygen. Electron beam parameters: $E_i = 2$ keV, $I = 2$ mA/cm^2.

was first cleaned by sputtering and annealing. The utilization of this procedure ensured that the Ni(111) substrate was not subjected to electron irradiation at any time during oxygen exposure.

When dosing oxygen without electron irradiation at 120 K, Fig. 1a, we find that following the initial chemisorption region there is very little further oxygen uptake, in contrast to earlier low temperature results [1]. Moreover, even for very long exposure times, the saturation level remains a factor of three lower than previously reported [1]. However, with electrons and oxygen simultaneously present we observe facile oxygen uptake, with a growth curve that reproduces previously reported low temperature oxygen incorporation data [1]. We also note that the

growth curve at 270 K without electron irradiation agrees quantitatively with previous findings for this system. This agreement at 270 K, in spite of the presence of significant electron fluxes in the prior studies [1–3], suggests that synergistic effects involving electrons which modify the kinetics of oxidation become much less important for this interface near room temperature [14]. A similar conclusion can be drawn from an earlier room temperature study [15] involving polycrystalline and (110)-oriented nickel. Our results in Fig. 1a convincingly demonstrate that facile oxide growth at low temperature is actually an effect stimulated by electron beam irradiation, and is not an inherent characteristic of the Ni(111) interface.

Data were also obtained by alternately exposing the sample to oxygen and then to a flux of electrons during Auger measurement of oxygen uptake. The oxygen flux was turned off during Auger data collection, ensuring that electrons and impinging oxygen were not present at the same time. The sample was then dosed with more oxygen and another Auger measurement subsequently taken. This process was continued until saturation. A comparison of the results obtained with simultaneous and alternating oxygen and electron exposures at 120 K is shown in Fig. 1b. These procedures yield identical oxygen uptake behavior.

The electron-stimulated effect we report here is quite robust, occurring over the entire range of incident electron beam energies examined, 5 eV to 2 keV. A more detailed study of energy-dependent cross sections will be presented elsewhere [14].

The saturated layers formed here with electron irradiation produce a 2 eV downward shift in the Ni 61 eV Auger peak, indicative of nickel oxide formation [16]. The oxide formed at 120 K does not produce NiO LEED spots, but only a Ni(111) LEED pattern with very strong diffuse background. This indicates that the oxide is largely disordered, probably consisting of many small domains. This differs from the combined NiO(111) and Ni(111) LEED spots generated by the 270 K grown material.

Perhaps the most informative characterization of the nickel/oxygen interfaces grown with various procedures comes from HREELS measurements. Fig. 2a shows a spectrum taken with oxygen dosed at $T_S = 120$ K without the presence of electrons. The

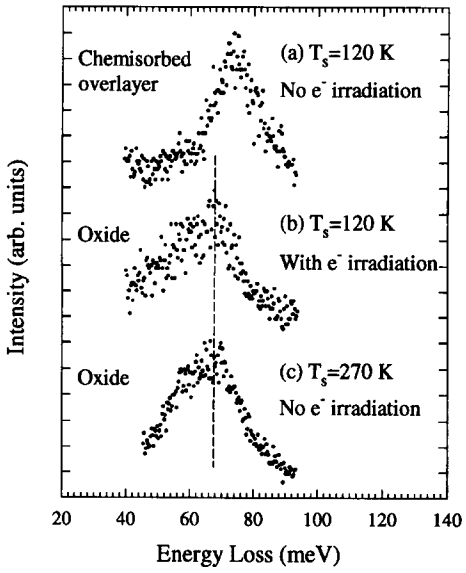

Fig. 2. Electron energy loss spectra after dosing oxygen by various procedures: (a) oxygen dosed at 120 K; (b) oxygen dosed at 120 K with electron irradiation; (c) oxygen dosed at 270 K. Spectrometer conditions: $E_i = 7$ eV with $\theta_i = \theta_f = 60°$; oxygen exposure = 36 L.

broad loss peak at about 73 meV can be assigned to the Ni–O stretch of atomically adsorbed oxygen [17,18]. Fig. 2b presents a spectrum obtained after the same oxygen exposure of a 120 K surface with the simultaneous presence of oxygen and 2 keV electrons. Note that several precautions were taken in order to assure that the HREELS spectrometer focussed on the same spot as was irradiated by the electron beam. Most importantly, we carefully mapped out the spatial extent of the electron-irradiated spot by systematically scanning the Auger spectrometer over the sample after it was oxidized in the presence of the electron beam. Using prior and precise spatial calibrations of the HREELS spot location, we could then aim the HREELS focal point to optimally overlap the electron-irradiated spot of the sample. Fig. 2c is for the same oxygen exposure with the surface held at 270 K without electron irradiation. Figs. 2b and 2c both show energy loss peaks at about 68 meV, a shift of 5 meV from the peak in Fig. 2a. (The perturbative effect of our HREELS spectrometer's electron beam is negligible due to its extremely low current density, 2.5 nA/cm^2.) Similar energy losses in HREELS spectra for NiO grown on

Ni(100) [19], and for NiO(100) and -(111) single crystals [20], have been assigned to a surface optical phonon of NiO. These experimental values are in good agreement with the calculated energy of 68.3 meV for the Fuchs–Kliewer surface phonon of nickel oxide [20]. We conclude that at 120 K and with electron irradiation we have formed 3 ML of NiO, whereas at 120 K and without electron irradiation essentially only chemisorbed oxygen is present, consistent with Fig. 1a.

Several key observations were considered in proposing a kinetic model for our results. Oxygen is known to adsorb dissociatively on Ni(111) above 20 K [21]. We have also shown that it is not necessary to simultaneously expose the target surface to both electrons and molecular oxygen in order to grow nickel oxide at 120 K, and, in fact, a single exposure of a chemisorbed oxygen overlayer to a 20 s dose of 2 keV electrons at 2 mA/cm^2 is sufficient to stimulate the growth of 3 ML of oxide upon subsequent oxygen exposure. Finally, we have found that electron irradiation of the clean Ni(111) surface using similar electron energies and currents does not promote low temperature oxidation. In light of these observations, we have ruled out electron-induced dissociation of chemisorbed molecular oxygen, gas phase oxygen/electron interactions, and electron beam damage of the substrate as possible mechanisms. Further, other authors have shown that similar electron exposures lead to negligible surface heating [10,11], thus ruling out thermal effects.

Starting with the above view we have developed a kinetic model which provides an excellent description of our results, based on the premise that electrons create nucleation centers around which nickel oxide islands form and grow. We assume that the number of nucleation centers, N, created by the electrons follows a differential rate law which, when integrated, yields:

$$\frac{N}{N_0} = 1 - \exp(-\phi_e \sigma t), \tag{1}$$

where N_0 is the saturation number of nucleation centers, ϕ_e is the electron flux density in electrons per cm^2 per second, t is electron exposure time, and σ is the (energy-dependent) cross section for the creation of nucleation centers by the electron beam.

Using a simple first-order kinetics model, we can describe the rate of nickel oxide growth as:

$$\frac{d\theta}{dt} = k(\theta_s - \theta)\frac{N}{N_0}, \tag{2}$$

where θ is the oxygen coverage, θ_S is saturation coverage, and k is the rate constant for oxide growth around the nucleation centers. Integrating Eq. (2), with N/N_0 given by Eq. (1), and subject to the initial condition $\theta = \theta_c$ at $t = 0$, where θ_c is the chemisorption saturation coverage and t is the oxygen exposure time, we have:

$$\theta = \theta_s - (\theta_s - \theta_c) \times \exp\left[-k\left(t + \frac{1}{\phi_e \sigma}\exp(-\phi_e \sigma t) - \frac{1}{\phi_e \sigma}\right)\right]. \tag{3}$$

We have compared the results predicted by Eq. (3) to experimental data collected by two complementary procedures. The first assesses the extent of oxide formation as a function of electron beam cur-

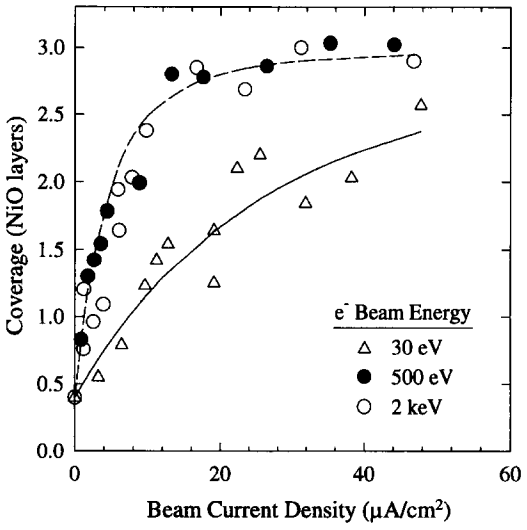

Fig. 3. Oxygen coverage versus electron beam current density with the sample at 120 K for constant oxygen exposure time, $t = 600$ s at $P_{ox} = 3 \times 10^{-8}$ Torr, using electron beam energies of 30, 500, and 2000 eV. Fits to the experimental data using the model given by Eq. (3) yield cross sections for electron-stimulated oxidation, see text.

rent density for fixed oxygen exposure. Fig. 3 presents the results for such a series of measurements for three different beam energies: 30, 500, and 2000 eV. Each data point in Fig. 3 was obtained by exposing the 120 K surface to a specified electron beam current density for 600 s in the presence of 3×10^{-8} Torr oxygen. (Auger intensities have been converted to nickel oxide coverage using a previously discussed electron escape depth correction [2].) Current densities have been corrected for the (rather small) changes which we measured in the electron beam spot size as a function of incident energy; spot sizes varied from 0.7 mm diameter for the highest energies used up to 0.9 mm at 30 eV. Non-linear least-squares fits of Eq. (3) to the data in Fig. 3, obtained by varying only the energy-dependent cross section for electron-stimulated oxidation, yield cross sections of 5×10^{-18} cm^2 for 30 eV (solid line), and 3×10^{-17} cm^2 for both 500 eV and 2 keV electrons (dashed line). These fits demonstrate that Eq. (3) provides an excellent description of the oxidation data as a function of electron beam current density.

Our model, using no adjustable parameters, can also quantitatively reproduce the oxygen uptake data obtained as a function of exposure time taken at several fixed electron beam current densities. Fig. 4 shows experimental oxygen uptake data taken with simultaneous oxygen and electron exposure using a 2 keV beam at current densities of 1.3, 9.8, and 2000 μA/cm^2. In the same figure, we also present the predictions from Eq. (3) using the cross section obtained from Fig. 3 for 2 keV electrons.

Work is underway to elucidate the nature and mechanism of production of these electron-induced nucleation centers. Recent studies have shown that oxide nucleation on Al(111) [22] and Mg(0001) [23] begins long before the saturation-chemisorbed coverage is reached. While our HREELS and AES results show that at an oxygen coverage of 0.4 ML on Ni(111) the oxygen is predominately chemisorbed, some small amount of NiO may also be present. There is evidence of molecular oxygen adsorption on NiO thin films grown on Ni substrates [24], and single crystals of NiO [25]. This would raise the possibility of a surface O_2^- species as an intermediate in the formation of these nucleation centers. Additionally, electronic excitation of adsorbed oxygen or a surface O^- species may be intermediates in

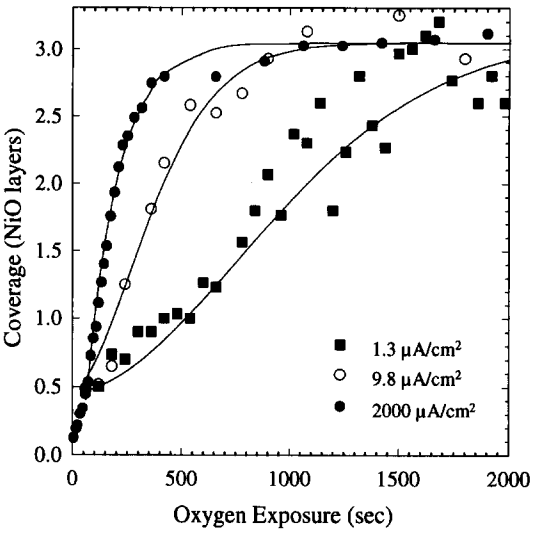

Fig. 4. Oxide growth versus time for three different electron beam current densities with the sample at 120 K, $E_i = 2$ keV and $P_{ox} = 3 \times 10^{-8}$ Torr. Solid lines are calculations generated from Eq. (3).

the formation of these nucleation centers. Finally, the presence of chemisorbed oxygen may weaken the bonding of surface Ni atoms, enhancing the cross section for defect creation by electron beams in the nickel surface. The similarity of the oxidation behavior with and without electron irradiation at room temperature suggests that the number of electron-created nucleation centers is a decreasing function of temperature, and our preliminary data indicates that these nucleation sites may be metastable [14]. We are also examining the role that secondary electrons may have in the creation of these nucleation centers [14].

In conclusion, we have demonstrated that synergistic effects involving incident fluxes of electrons can greatly modify the oxidation behavior of Ni(111) at low temperature. We have also shown that in the absence of such electrons nickel oxide grows much more slowly than had been previously reported for this important interface. A kinetic model has been proposed which quantitatively reproduces the electron-stimulated oxidation data and yields the energy-dependent cross sections for this phenomenon.

Acknowledgements

This work was supported by the Air Force Office of Scientific Research and, in part, by the MRSEC Program of the National Science Foundation under Award Number DMR-9400379.

References

[1] P.H. Holloway and J.B. Hudson, Surf. Sci. 43 (1974) 141.
[2] P.H. Holloway and J.B. Hudson, Surf. Sci. 43 (1974) 123.
[3] P.R. Norton, R.L. Tapping and J.W. Goodale, Surf. Sci. 65 (1977) 13.
[4] H. Hopster and C.R. Brundle, J. Vac. Sci. Technol. 16 (1979) 548.
[5] W. Wang, N. Wu and P.A. Thiel, J. Chem. Phys. 92 (1990) 2025.
[6] A.G. Fedorus, V.V. Gouchar, I.V. Kanash, E.V. Klimenko, A.G. Naumovets and I.N. Zasimovich, Surf. Sci. 251/252 (1991) 846.
[7] R. Ramsier and J.T. Yates, Jr., Surf. Sci. Rep. 12 (1991) 243.
[8] Y. Margoninski, D. Segal and R.E. Kirby, Surf. Sci. 51 (1975) 488.
[9] C. Xu and B.E. Koel, Surf. Sci. 292 (1993) L803.
[10] H.J. Jänsch, J. Xu and J.T. Yates, Jr., J. Chem. Phys. 99 (1993) 721.
[11] J.M. Fontaine, O. Lee-Deacon, J.P. Duraud, S. Ichimura and C. Le Gressus, Surf. Sci. 122 (1982) 40.
[12] Y. Chen, Y. Luo, J.M. Seo and J.H. Weaver, Phys. Rev. B 43 (1991) 4527.
[13] W. Menezes, P. Knipp, G. Tisdale and S.J. Sibener, Phys. Rev. B 41 (1990) 5628.
[14] M.J. Stirniman, Wei Li and S.J. Sibener, submitted.
[15] J. Verhoeven and J. Los, Surf. Sci. 58 (1976) 566; J. Verhoeven, in: Proc. IVC-7 & ICSS-3 (Vienna, 1977) p. 915.
[16] A.M. Horgan and I. Dalins, Surf. Sci. 36 (1973) 526.
[17] H. Ibach and D. Bruchmann, Phys. Rev. Lett. 44 (1980) 36.
[18] G. Tisdale and S.J. Sibener, Surf. Sci. 311 (1994) 360.
[19] G. Dalmai-Imelik, J.C. Bertolini and J. Rousseau, Surf. Sci. 63 (1977) 67.
[20] P.A. Cox and A.A. Williams, Surf. Sci. 152/153 (1985) 791.
[21] J.D. Beckerle, Q.Y. Yang, A.D. Johnson and S.T. Ceyer, Surf. Sci. 195 (1988) 77.
[22] H. Brune, J. Wintterlin, J. Trost, G. Ertl, J. Wiechers and R.J. Behm, J. Chem. Phys. 99 (1993) 2128.
[23] P.A. Thiry, J. Ghijsen, R. Sporken, J.J. Pireaux, R.L. Johnson and R. Caudano, Phys. Rev. B 39 (1989) 3620.
[24] S.J. Bushby, T.D. Pope, B.W. Callen, K. Griffiths and P.R. Norton, Surf. Sci. 256 (1991) 301.
[25] A.A. Tsyganenko, T.A. Rodionova and V.N. Filimonov, React. Kinet. Catal. Lett. 11 (1979) 113.